

7th International Conference on Silicon Photovoltaics, SiliconPV 2017

Oxygen-related defects in n-type Czochralski silicon wafers studied by hyperspectral photoluminescence imaging

Torbjørn Mehl^{a,*}, Ingunn Burud^a, Elénore Letty^b and Espen Olsen^a

^aNorwegian University of Life Sciences, NMBU, Universitetstunet 3, 1433 Ås, Norway

^bCEA, LITEN, INES-Department of solar technologies, F-73375 Le Bourget du Lac, France

Abstract

Oxygen-related Thermal Donors in n-type Czochralski silicon (Cz-Si) wafers have been investigated using hyperspectral photoluminescence imaging and OxyMap. Thermal Donors give rise to two photoluminescence emissions, one narrow peak at 0.767 eV, and one broad band with centre peak at 0.72 eV that is also measurable at room temperature. The spectral imaging was first carried out on the sample cooled to 90 K, then repeated at room temperature (300 K). The possibility to delimitate at room temperature defects-rich zones with hyperspectral photoluminescence imaging is evidenced.

© 2017 The Authors. Published by Elsevier Ltd.

Peer review by the scientific conference committee of SiliconPV 2017 under responsibility of PSE AG.

Keywords: hyperspectral imaging; photoluminescence; thermal donor; oxygen; Czochralski silicon

1. Introduction

Oxygen is a major impurity in Czochralski (Cz) Si. It comes from the dissolution of the quartz crucible during crystallization and is incorporated in large amount in the ingot. Interstitial oxygen (O_i) has not been shown to be recombination active so far, but it gives birth to multiple defects. This is for example the case of oxide precipitates formed at high temperature and responsible for efficiency losses of more than 4 % absolute [1]. This is also the case of Thermal Donors (TD) which are electrically active clusters of Si and O_i formed at temperatures in the range 350–550°C. TD are known to be recombination-active and to introduce multiple energy levels into the gap [2].

* Corresponding author. Tel.: +47-98446844.

E-mail address: torbjorn.mehl@nmbu.no

The existence of intermediate energy levels in the gap may enable recombination pathways for photo excited charge carriers. This pathways can be radiative or non-radiative. In general freeze out of phonons in indirect bandgap semiconductor like Silicon will cause more and more processes to be of radiative nature, due to energy conservation as the sample temperature is lowered towards cryogenic temperature.

Several lines in the photoluminescence (PL) spectra have been observed and linked to oxygen-related defects such as TD. Especially the P and H lines have been reported by many [3-6] to be connected to TD. The photon energy of the zero-phonon line of P is 0.767 eV and for H 0.926 eV. The P line is observed in samples with oxygen concentration above $3\text{--}5 \times 10^{17} \text{ cm}^{-3}$ [7] regardless if it is n- or p-type doped silicon [3]. Tajima [8] reports a broad PL emission band with center energy 0.7 eV accompanying the P line. While the 0.7 eV band is observable at room temperature, the P line is visible only below 150 K. The H line has been associated with a TD defect complex involving both oxygen and carbon [6].

Hyperspectral PL imaging has been used in previous studies to characterize multicrystalline silicon wafers and solar cells [9-13], but the technique have never before been used on Cz-Si wafers.

In this study, the aim was to determine the potential of hyperspectral PL imaging to detect heterogeneous distribution of defects/impurities in Cz wafers. Areas full of O_i related defects will be particularly studied not only at low temperatures but also at room temperature.

2. Materials and method

The sample characterized in this study is a wafer from an n-type, phosphorus doped, Czochralski ingot. The 156 mm x 156 mm wafer is from the top part (seed-end) of an industrial ingot, solidified fraction < 5%. This part contains the highest $[O_i]$ and is submitted to a rather slow cooling. It should thus contain high densities O_i -related defects. The as-cut resistivity is stated to vary from 1.5 Ωcm at the wafer center to 5 $\Omega\text{.cm}$ at the edge related to a high variation of [TD] across the wafer diagonal. The wafer was chemically textured (KOH) in order to remove the saw damaged layer. We are therefore confident that the PL imaging presented in these study are representative of the bulk of the wafer

The $[O_i]$ was determined by OxyMap on a sister wafer. This characterization tool aims at measuring $[O_i]$, [P] and as-grown [TD] across the wafers. It is based on resistivity measurements on as-received wafers, after controlled generation of TD and after suppression of TD. Details about the technique can be found in [14].

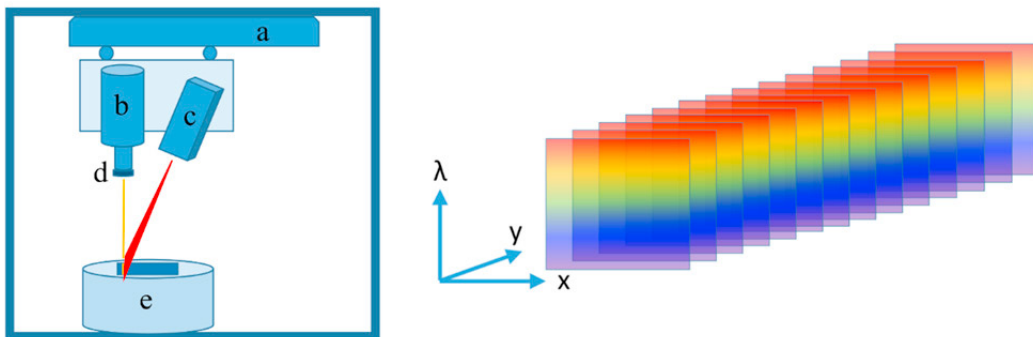


Fig. 1. Hyperspectral imaging setup. a) translation stage, b) hyperspectral camera, c) line laser, d) low pass filter and e) cryogenic cooler. The camera records a 2D image with one spatial and one spectral dimension. The second spatial dimension is obtained by assembling images taken while the camera scans the sample using the translation stage.

In this study a hyperspectral photoluminescence imaging setup, shown in Fig. 1, have been used. The near-infrared (NIR) push-broom hyperspectral camera, with a mercury cadmium telluride detector (MCT), has a spectral resolution of 6nm in the range 930–2500 nm (0.49–1.13 eV). As excitation source, an 808 nm line laser was used with an irradiated power density of 2 W/cm² (Lasiris Magnum II). A 1000 nm low-pass filter prevented laser beam reflections from entering the optic apparatus. The camera records a 2D image with one spatial, (x), and one spectral

dimension, (λ). By assembling images taken while the camera scans the sample, one gets a second spatial dimension, (y). This provides a PL spectrum in each spatial pixel(x,y) of the sample. In the setup for this study, the spatial resolution is 250 μm . Images are taken of the samples at room temperature, 300 K, and of the samples cooled with liquid nitrogen to 90 K. A similar setup has been used in previous studies [9-13]. The scanning speed for PL mapping was approximately 0.6 cm s^{-1} for the spatial resolution used in this study.

A tool to separate PL of different origins, even though they have overlapping spatial distribution and/or PL spectrum, is multivariate curve resolution analysis (MCR) [15]. The mathematical method uses multivariate statistics for deconvolving complex, convoluted signals composed of several discrete, simultaneously occurring signals and can be represented mathematically by Eq. (1):

$$D = CS^T + E$$

MCR decomposes the measured data, matrix D , into a number of representative scores in matrix S^T , with the corresponding loading vectors in matrix C . An alternating least squares (ALS) algorithm is used to minimize the error matrix, E . The different radiative components are manifested with images of the spatial distribution in S^T and their corresponding spectrum in C . In this study, the MCR algorithm in PLS_Toolbox version R8.2.1 (Eigenvector Research, Inc., USA) running on MATLAB R2016b (The MathWorks, Inc., USA) was used.

3. Results and discussion

OxyMap measurements of the sample give the O_i distribution along the wafer diagonal shown in Fig. 2. The O_i

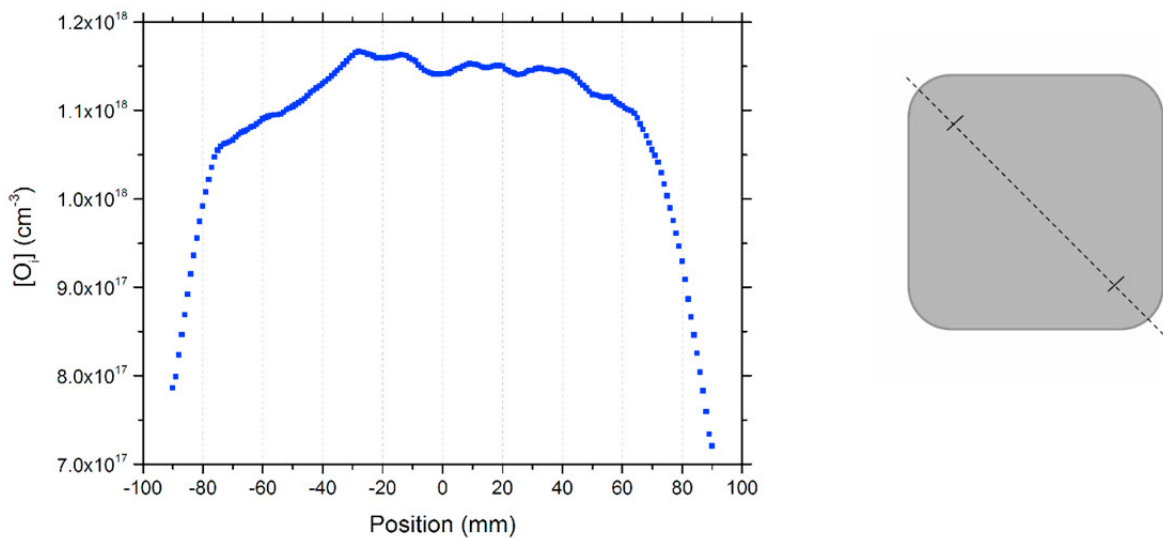


Fig. 2. Concentration of interstitial oxygen distribution along the wafer diagonal.

content was found to be around $1.1 \times 10^{18} \text{ cm}^{-3}$, higher in the centre of the wafer and decreasing towards the wafer edge. The distribution of TD across the wafer diagonal is very similar (not shown here), with higher [TD] at wafer centre, since it is greatly dependent on $[O_i]$.

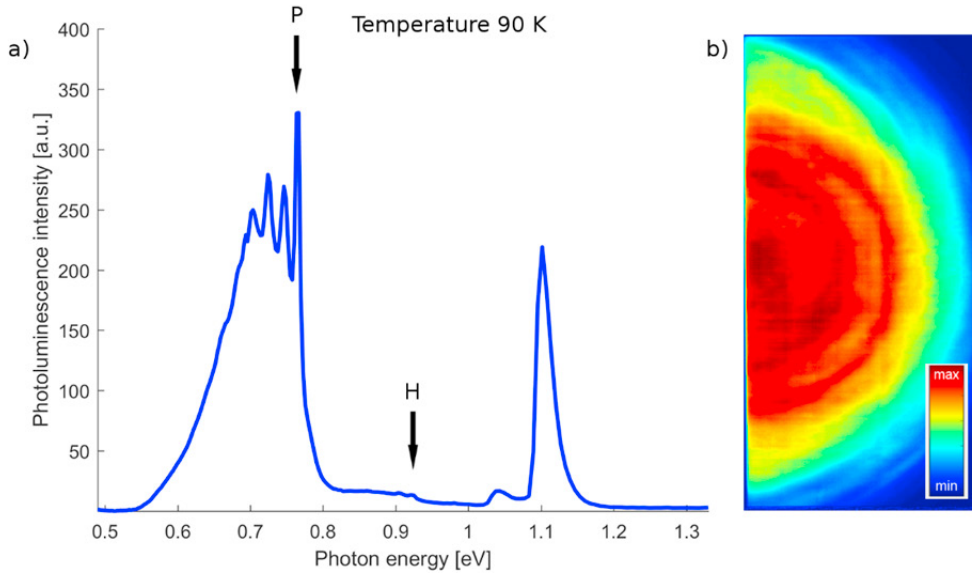


Fig. 3. (a) Photoluminescence spectrum from a textured cz-Si n-type wafer at T = 90 K. P and H lines marked. (b) Image from the integral of defect related photoluminescence, range 0.66–0.77 eV

The hyperspectral PL spectrum, integrated over the entire surface of the Cz-Si n-type wafer, cooled to 90 K, is shown in Fig. 3a). The low intensity in the band-to-band PL, at 1.10 eV, could either be due to rapid recombination of photoexcited charge carriers due to high surface recombination in the unpassivated sample or due to enhanced recombination caused by a high oxygen content. A weak signal from the H line is found at 0.926 eV. If looking at the defect related PL as a single entity, it gives rise to a broad band with peak centred at 0.72 eV. This broad band also has local sharp peaks. The one with highest energy is the P line at 0.767 eV. Other local peaks are at 0.746 eV, 0.724 eV, 0.704 eV and shoulders at 0.789 eV, 0.684 eV and 0.666 eV. The spatial distribution of the defect related PL is given in Fig. 3b). The pattern is ring-like and strongest in the centre. This correlates well with the concentration of O_i (Fig. 2) and TD.

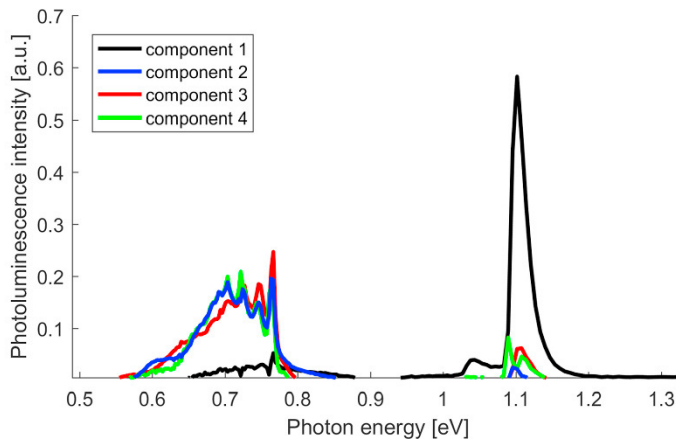


Fig. 4. MCR analysis only manage to separate the band-to-band PL from the TD related PL.

To investigate the spatial distribution of the various local peaks, MCR was used. MCR analysis did not divide the TD related PL into different signals, neither spatial nor spectral. Only the band-to-band signal was separated (Fig. 4). This indicates that all peak energy levels are present simultaneously from the defects in this wafer.

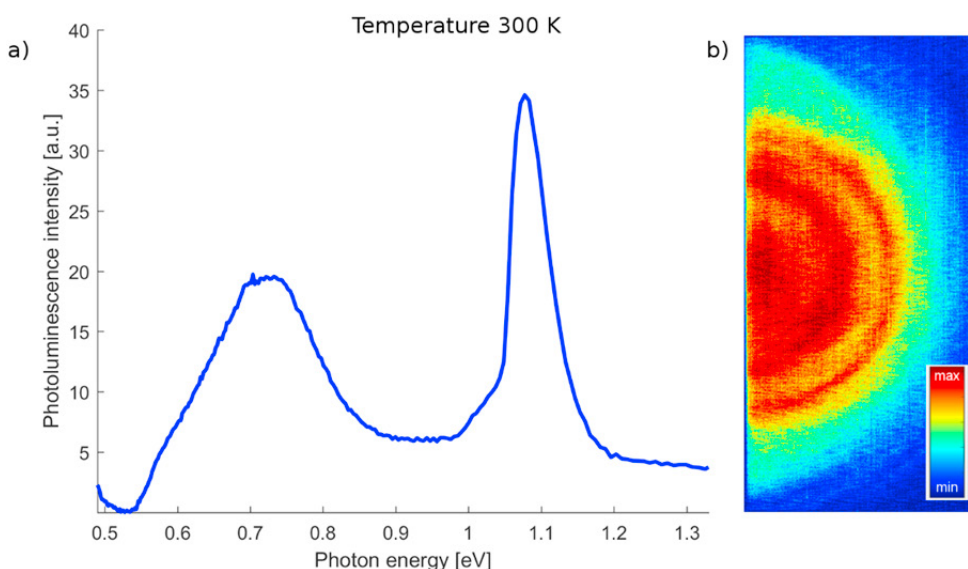


Fig. 5. Hyperspectral PL imaging at room temperature. a) Photoluminescence spectrum from a textured Cz-Si n-type wafer at $T = 300\text{K}$. b) Image from the integral of defect related photoluminescence, range 0.66–0.77eV.

Since the P line is related to TD, it can be assumed that the rest of the broad band with center at 0.72 eV also is related to TD. The different energy levels can be due to phonon replicas and/or TD with different oxygen–silicon complexes.

The results from the measurement at 300 K are shown in Fig. 5. The band-to-band PL has shifted from a sharp peak at 1.10 eV in the cooled (90 K) wafer to a broader peak with center at 1.08 eV for the sample at 300 K. This corresponds to the narrowing of bandgap with higher temperature [16]. There is also a broad PL signal with center peak at 0.72 eV, without any significant local peaks. Neither is the P line seen, as expected since the temperature is higher than 150 K. Nor is the H line detected.

The spatial distribution of the 0.72 eV signal is shown in Fig. 5 b). Even though the PL signal is weaker and has lower signal to noise ratio, the spatial distribution corresponds with the measurement obtained at 90 K, and therefore has the same origin. It is not possible to detect, from this dataset, if the peak center is shifted towards lower energies due to higher temperature.

4. Conclusion

As expected from the literature, the P line at 0.767 eV was observed in the areas full of TD at low temperature. This line was accompanied by the broad band with centre peak at 0.72 eV that can also be detected at room temperature. Hyperspectral PL imaging seems thus a promising tool to detect heterogeneous distribution of defects also in Czochralski Si.

Very few trap-assisted recombinations are radiative at room temperature. The most studied is the D1 (at 0.807 eV) defect line [17], and the broad defect emission band at 0.72 eV has previously been detected at room temperature [8]. The emission strength of this 0.72 eV band is comparable to the band-to-band PL signal. This indicates that these mechanisms can be used for a variety of applications, such as up conversion of photons, light emitting diodes and classifications of wafers.

The origin of the local peaks within the 0.72 eV signal at 90 K should be a topic for further studies.

References

- [1] Haunschild, J., et al., Detecting efficiency-limiting defects in Czochralski-grown silicon wafers in solar cell production using photoluminescence imaging. *Physica Status Solidi-Rapid Research Letters*, 2011. 5(5-6): p. 199-201.
- [2] Tomassini, M., et al., Recombination activity associated with thermal donor generation in monocrystalline silicon and effect on the conversion efficiency of heterojunction solar cells. *Journal of Applied Physics*, 2016. 119(8): p. 084508.
- [3] Pizzini, S., et al., The photoluminescence emission in the 0.7-0.9 eV range from oxygen precipitates, thermal donors and dislocations in silicon. *Journal of Physics-Condensed Matter*, 2000. 12(49): p. 10131-10143.
- [4] Minaev, N. and A. Mudryi, Thermally - induced defects in silicon containing oxygen and carbon. *physica status solidi (a)*, 1981. 68(2): p. 561-565.
- [5] Uozumi, Y. and T. Katoda, Effects of stress on generation of P-line defects near insulator-silicon interface. *Applied surface science*, 1997. 117: p. 624-628.
- [6] Tajima, M., P. Stallhofer, and D. Huber, Deep Level Luminescence Related to Thermal Donors in Silicon. *Japanese Journal of Applied Physics*, 1983. 22(9A): p. L586.
- [7] Wagner, P. and J. Hage, Thermal double donors in silicon. *Applied Physics A*, 1989. 49(2): p. 123-138.
- [8] Tajima, M., Characterization of semiconductors by photoluminescence mapping at room temperature. *Journal of Crystal Growth*, 1990. 103(1-4): p. 1-7.
- [9] Olsen, E. and A.S. Flo, Spectral and spatially resolved imaging of photoluminescence in multicrystalline silicon wafers. *Applied Physics Letters*, 2011. 99(1): p. 3.
- [10] Burud, I., et al., Hyperspectral photoluminescence imaging of defects in solar cells. *Journal of Spectral Imaging*, 2016. 5.
- [11] Lausch, D., et al., Classification of crystal defects in multicrystalline silicon solar cells and wafer using spectrally and spatially resolved photoluminescence. *Journal of Applied Physics*, 2016. 119(5).
- [12] Mehl, T., et al., Defects in multicrystalline Si wafers studied by spectral photoluminescence imaging, combined with EBSD and dislocation mapping. *Proceedings of the 6th International Conference on Crystalline Silicon Photovoltaics (Siliconpv 2016)*, 2016. 92: p. 130-137.
- [13] Flo, A., et al., Distribution of radiative crystal imperfections through a silicon ingot. *Aip Advances*, 2013. 3(11): p. 9.
- [14] Veirman, J., et al., Oxygen-defect characterization for improving R&D relevance and Cz-Si solar cell efficiency. *Photovoltaics International*, 2016. 33.
- [15] Tauler, R., Multivariate curve resolution applied to second order data. *Chemometrics and Intelligent Laboratory Systems*, 1995. 30(1): p. 133-146.
- [16] A. Schenk, Finite-temperature full random-phase approximation model of band gap narrowing for silicon device simulation, *Journal of Applied Physics*, 84 (7), pp. 3684–3695, 1998.
- [17] Koshka, Y., et al., Scanning room-temperature photoluminescence in polycrystalline silicon. *Applied physics letters*, 1999. 74(11): p. 1555-1557.